Alrekabi, T.Kh., Cunha, V.M.C.F., Barros, J.A.O., Reactive powder concrete reinforced with steel fibres exposed to high temperatures (2017) IOP Conference Series: Materials Science and Engineering, 246 (1), art. no. 012020, DOI: 10.1088/1757-899X/246/1/012020

Reactive powder concrete reinforced with steel fibres exposed to high temperatures

T Kh Alrekabi [1,3], **V M C F Cunha** [2,4] **and J A O Barros** [2,5]

[1] Architecture Engineering Department, Engineering Faculty, Koya University, University Park, Danielle Mitterrand Boulevard, Koysinjaq KOY45, Iraq.
[2] ISISE, Department of Civil Engineering, School Eng., University of Minho, Campus de Azurém, 4800-058 Guimarães, Portugal.

[3] taghreed.khaleefa@koyauniversity.org, [4] vcunha@civil.uminho.pt,
[5] barros@civil.uminho.pt

Abstract. An experimental investigation was carried out to assess the mechanical properties of reactive powder concrete (RPC) reinforced with steel fibres (2% in vol.) when exposed to high temperatures. The compressive, flexural and tensile strength, modulus of elasticity and post-cracking behaviour were assessed after specimens' exposure to different high temperatures ranging from 400 to 700ºC. The mechanical properties of the RPC were assessed for specimens dried for 24 hours at 60 ºC and 100 ºC. Partially dried specimens (60 ºC) exhibited explosive spalling at nearby 450 ºC, while fully dried RPC specimens (100 ºC) maintained their integrity after heating exposure. In general, the mechanical properties of RPC significantly decreased with the increase of the temperature exposure. The rate of decrease with temperature of the compressive, tensile and flexural strengths, as well the corresponding post-cracking residual stresses was higher for exposure temperatures above the 400 ºC.

1. Introduction

Since the appearance of the reactive powder concrete (RPC) in the early 90's, significant research has been carried out to develop and characterize this material. RPC is characterized by having very low water to binder ratio (W/B), and very dense microstructure formed by using a combination of powders including cement, silica fume, and ground quartz sand, as well by excluding the coarse aggregates from its composition. This combination endows RPC of ultra-high strength and high durability [1, 2]. When heat-treatment and/or pre-setting pressurization are used, RPC may attain compressive strengths ranging from 200 to 800 MPa [3, 4]. However, the high strength of RPC makes it extremely brittle; therefore, commonly fibres are added into the mixture (ranging from 1.5 to 3% in vol.) in an attempt of decreasing its brittleness [5].

RPC may be used on an assortment of applications, such as prestressed concrete structures, nuclear power plants, large-span arch roof structures and bridges and in structural rehabilitation. Within these structural applications, fire poses a tangible possible hazard. The potential risk of structural collapse due to fire resides in the highly brittle nature of RPC. Nevertheless, up to now, research on the fire / elevated temperatures exposure resistance of RPC is still scarce. Numerical investigations revealed that RPC is prone to explosive spalling under high temperature [6-8]. Moreover, experimental investigations [9] found that RPC spalled under high temperatures in a distinct manner than that of

high-strength or high-performance concrete. Nonetheless, the spalling mechanisms of RPC still remain unknown. Liu and Huang [9] conducted a series of fire resistance tests and found that the residual compressive strength of RPC decreased with increasing fire duration.

This work presents and discusses the results of an experimental program to assess the mechanical properties of RPC reinforced with steel fibres (2% in vol.) when exposed to high temperatures. The compressive, flexural and tensile strength, modulus of elasticity and post-cracking behaviour were assessed after specimens' exposure to different high temperatures ranging from 400 to 700 ºC.

2. Experimental Program

2.1. Materials and concrete composition

The materials used in the production of the RPC were: cement, fine sand, silica fume, superplasticizer, tap water and steel fibres. Table 1 includes the final RPC composition per cubic metre. This mixture was selected after carrying out 9 preliminary trial batches. The guidelines given in [10] were adopted for fixing the quantity of cement, fine sand, and steel fibres. On the other hand, the quantities of silica fume, super-plasticizer and water were varied in order to obtain a mixture with proper rheological and mechanical properties, as well an adequate fibre distribution.

Table 1. RPC composition per m^3.

Cement [kg]	Fine sand [kg]	Silica fume [kg]	Superplasticizer [kg]	Water [kg]	Fibres [kg]
1000	1000	150	21.25	212.5	156

An ordinary Portland cement CEM I 42.5R produced by the Cement Company SECIL was adopted. Fine aggregates were used exclusively, namely, a natural river sand (non-siliceous), which was already clean and nearly free from impurities. The fine sand maximum nominal size was about 1 mm, which makes it suitable to be used in the production of RPC [11]. Figure 1 shows the grading of the adopted fine sand. Note that all the retained particles in the sieve with an opening of 1 mm were discarded, in spite of being very few.

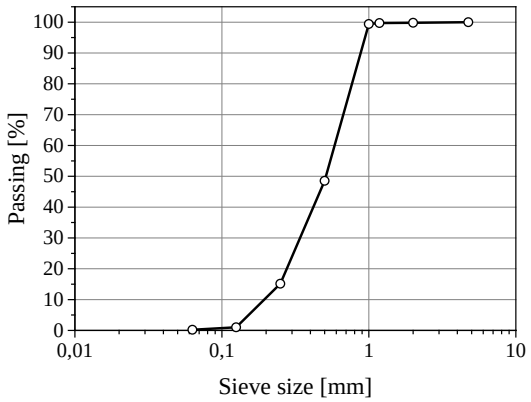

Figure 1. Grading of fine sand.

A greyish colored densified silica fume was used as an addition in the RPC mixes to enhance mainly the matrix densification. A superplasticizer commercially available, specifically Sika ViscoCrete® 20HE, was used as a high performance high water reducer admixture to produce the RPC. The solid content of this superplasticizer was 40% and its density was 1.08 kg/l. Tap water was used both for the mixture and curing of the specimens. Finally, high strength straight steel fibers with a copper coating and an aspect ratio (l_f/d) of 30 were used in all RPC mixtures. Table 2 includes the main properties of the used fibres.

Table 2. Geometric and mechanical properties of the steel fibres.

Length [mm]	Diameter [mm]	Tensile strength [MPa]	(l_f/d) [-]	Conformity standard
6	0.2	2800	30	ASTM-A820

2.2. Concrete mixture and curing procedures

The mixture procedure was performed using a rotary mixer with a capacity of 6 litters. Firstly, sand and cement were introduced into the mixer, respectively, and then mixed during 3 minutes. Afterwards, silica fume was added and mixed with the other constituents for more 3 minutes. Superplasticizer was added into the water jar and then stirred. This mixture was slowly added to the pre-mixed aggregates and binder into the mixer. After the addition of the total water and superplasticizer, the mixture procedure was carried out for more 3 minutes. The mixing process was stopped to remove and remix by hand any material bonded to the mixer's walls and flat beater, and then restarted for three additional minutes. This step was repeated until the mixture exhibited a good homogeneity. Finally, steel fibres were added slowly by hand during the mixing. The total mixing time was about 18 to 24 minutes.

The moulds were filled with the RPC mixture, and then vibrated during approximately 1 minute on a vibration table. After casting, all moulds were covered with a wet cloth for 48 hours to minimize the loss of moisture. Finally, after the 48 hours, the specimens were unmoulded and submerged under water in a climate chamber at a 20 ºC temperature and 98% relative humidity until testing age, at about 28 days.

2.3 Exposure to high temperatures procedure

Prior to the exposure to the high temperatures procedure and mechanical testing, specimens were dried under two distinct moderate temperatures for about 24 hours, respectively, at 60 and 100 ºC. This aimed to check the influence of the specimens' moisture degree on the eventual explosive spalling of the specimens under high temperatures. The moisture degree was only assessed in some prismatic specimens and revealed that at 100 ºC the specimens were fully dried, whereas in specimens dried at 60 ºC the core of the prismatic specimens was still wet. In the latter specimens, the average decrease of specimen's weight after dried at 100 ºC was 7%.

An electric furnace with a maximum temperature of 1200 ºC was used to subject the specimens to temperatures of, respectively, 400, 500, 600 and 700 ºC. The heating and exposure procedures were similar for all the target temperatures. A heating rate of 10 ºC/min up to the target temperature was maintained constant. After attaining the desired target temperature, the specimens were maintained at a constant temperature for one hour. Finally, specimens were allowed to gradually cool down over more than 24 hours. The cooling speed was slightly different for every target temperature. The temperature of all specimens was the same room temperature at the time of testing.

Table 3 includes the number of specimens that spalled when submitted to the high temperatures exposure for each drying condition. Additionally, it is included in round brackets the total number of specimens that have been exposed to each target temperature and drying conditions. Note that some specimens even though may not exhibited a visible failure pattern, most probably had severe micro-cracking due to damage induced by the thermal stresses gradient.

Table 3. Failure of specimens due to high temperatures exposure for distinct drying conditions.

Temp. Exposure		400 ºC		500 ºC		600 ºC		700 ºC	
Drying Temp.		60 ºC	100 ºC	60 ºC	100 ºC	60 ºC	100 ºC	60 ºC	100 ºC
Specimens	Compression	-	0 (4)	-	0 (4)	-	0 (4)	-	0 (2)
	Tension	0 (4)	-	2 (4)	-	4 (4)	-	-	-
	Flexure	0 (4)	-	4 (4)	-	3 (4)	-	-	0 (2)

The totality of specimens that have been exposed to 400 ºC for one hour did not suffered any spalling damage when dried at 60 ºC. Moreover, the specimens dried at 100 ºC also did not exhibit spalling, for 500, 600 and 700 ºC. The explosive spalling occurred for specimens dried at 60 ºC, consequently in the presence of moisture inside the specimen. The specimen failure was clearly audible in the laboratory due to the strong explosion of the specimens. This explosion occurred at nearby 450 ºC, which is in accordance with other research carried out for high strength concretes under high temperatures [12-13]. The latter occurrence maybe ascribed by the dehydration of the calcium hydroxide that occurs from 400 to 550 ºC, which could increase the build-up of high pore pressure [14]. Figure 2 depicts some examples of the observed specimen failure when submitted to high temperatures.

Figure 2. Failure due to high temperature: (a) and (b) spalling at 500 ºC of direct tension and flexure specimens, respectively; (c) cracking of direct tension specimen at 600 ºC, and (d) spalling of flexure specimens at 600 ºC.

2.4. Test set-up and specimen geometry

A total of 52 specimens with distinct geometries were cast for performing compressive, flexural and uniaxial tensile tests. In general, four specimens per each series corresponding to a test typology and temperature exposure were used with the exception of the 700 ºC series. In the subsequent sections the specimen geometry and corresponding test set-up are described.

2.4.1. Compression tests. Cylindrical specimens with an approximate diameter of 44 mm and 105 mm height were employed for assessing the elasticity modulus and the compressive stress - strain relationship. Prior to testing, both top and bottom surfaces of all cylinders were carefully grinded to ensure plane and parallel surfaces. It was always guaranteed a height to diameter ratio higher than 2.

In a first stage, the test to determine the static modulus of elasticity was carried out under force control over a certain number of cycles. In the loading cycle, the stress was applied at a velocity of 0.2 MPa/s until a stress level of one third of the compressive strength is attained. The test ended when the strain difference, between two consecutive loading cycles, did not exceed 1×10^{-5}, according to [15]. Figure 3(a) shows the adopted set-up for the test of modulus of elasticity. On the other hand, the compressive stress-strain relationship of the developed RPC was obtained according to the test set-up depicted in figure 3(b). The latter test was carried out with closed-loop displacement control at a rate of 10 μm/s. The specimen's displacement was computed from the average readings of three LVDTs measuring the relative displacement the frame's rigid steel plates. Then, the strain was found by divided the average displacement on the length of the specimen.

(a) (b)

Figure 3. Compression tests set-up for determining the: (a) modulus of elasticity, (b) stress – strain relationship.

2.4.2 Uniaxial tensile tests. The tensile tests were carried out on dog-bone shaped specimens. The geometric details of the specimen are shown in the figure 4(a), whereas the test set-up is depicted in figure 4(b). The specimen deformation was obtained from the average readouts of two LVDTs with a gauge length of 120 mm. The tests were performed under closed-loop displacement control at a rate of 5 μm/s. The specimens were carefully fastened to the grips before testing, nevertheless after having been submitted to high temperatures, the specimens were slightly warped maybe due to the thermal stress gradient induced during the heating procedure. This may have introduced some damage in these specimens during their fixing process to the grips, which may have contributed to decrease their tensile strength.

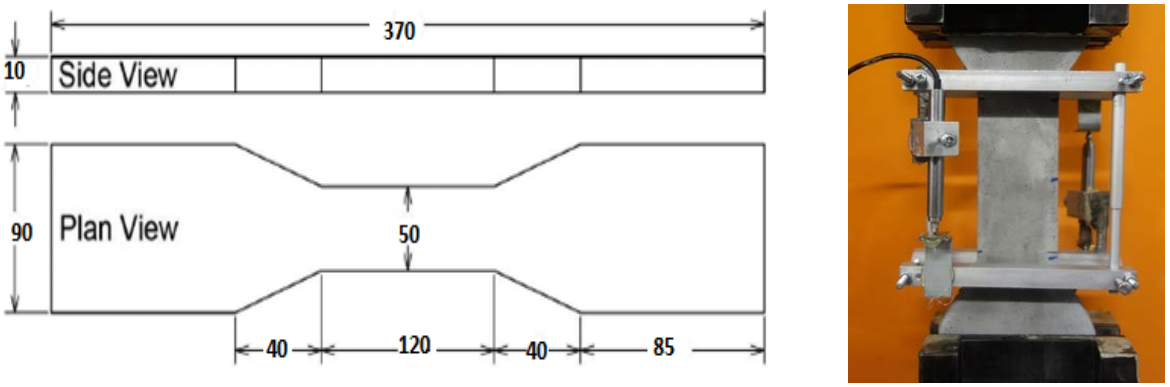

(a) (b)

Figure 4. (a) Dog-bone specimen (dimensions in mm), (b) uniaxial test set-up (dimensions in mm).

2.4.3 Three-point bending test. RPC prismatic specimens of 40×40×160 mm were prepared before testing. A notch at the mid-length of the prism with a depth of 1/4 times of the beam height (i.e. 10 mm) and a width of 1 mm was executed in the lateral surface all specimens, i.e. on a surface parallel to the casting direction. The loading span was 150 mm. Figure 5 shows the adopted test set-up. The tests were performed under closed-loop displacement control at a rate of 5 μm/s. One LVDT was used to assess the deflection at mid-span, figure 5(a), whereas the other one was used to obtain the crack mouth opening displacement, figure 5(b).

(a) (b)

Figure 5. Three-point bending test set-up: (a) view of full length of specimen, (b) crack mouth opening displacement measurement.

3. Experimental results

Table 4 resumes the main results obtained for the mechanical properties of the RPC tested under distinct high temperatures, namely, the average (Avg.) and coefficients of variation (CoV) for each.

Table 4. Main mechanical properties of the RPC exposed to high temperatures.

Temperature	Compressive strength [MPa]		Modulus of elasticity [GPa]		Tensile strength [MPa]		Flexural strength [MPa]	
	Avg.	CoV	Avg.	CoV	Avg.	CoV	Avg.	CoV
20 ºC	137.6	4.8%	46.48	10.3%	4.8	28.8%	20.9	9.5%
400 ºC	102.2	1.5%	30.9	5.8%	4.1	15.4%	15.4	14.0%
500 ºC	84.4	1.2%	22.3	18.0%	3.6	-	-	-
600 ºC	68.2	10.5%	17.5	7.2%	-	-	8.6	-
700 ºC	65.4	5.2%	18.4	4.7%	-	-	1.0	13.9%

Figure 6 depicts the variation of the compressive strength, f_{cm}, modulus of elasticity, E_{cm}, flexural strength (normal stress under flexure), f_{fm}, and tensile strength, f_{tm}, with the high temperatures that specimens have been exposed.

Both the compressive strength and modulus of elasticity decreased approximately in a linear fashion up to a temperature of 600 ºC and no significant variation was observed when increasing the temperature to 700 ºC. The slight increase of the modulus of elasticity as well the slight decrease for the compressive strength, when increasing the temperature from 600 to 700 ºC, is within the expected experimental scatter of this kind of material. Thus it can be concluded that the damage level of the matrix for those two temperatures would be similar. For an exposure temperature of 600 ºC the reduction on the compressive strength and elasticity modulus when compared to the one obtained for room temperature was about 50 and 62%, respectively.

A significant decrease on the flexural strength with the increase of temperature was observed up to 700 ºC. The variation was markedly nonlinear, and a steeper decrease of the flexural strength was observed after the 400 ºC. The reduction of the flexural strength of specimens exposed to 600 and 700 ºC when compared to the one obtained at room temperature was about 60 and 95%, respectively. On the other hand, the tensile strength revealed a slight decrease with temperature, however, since only it was possible to test specimens exposed up to 500 ºC no definite conclusions can be withdraw.

3.1. Compressive stress-strain relationships

Figure 7 shows the average compressive stress-strain relationships of the RPC specimens exposed to the distinct high temperatures. It is clearly visible the decrease on the inclination of the pre-peak branch with the increase of temperature corresponding to a decrease of the matrix stiffness due to the thermal induced damage. Regarding the post-peak branch it is also noticeable a decrease on the

residual strength with the increase of temperature. In particular, for temperatures above 600 ºC, and for deformations higher than 0.01 the residual strength was practically null.

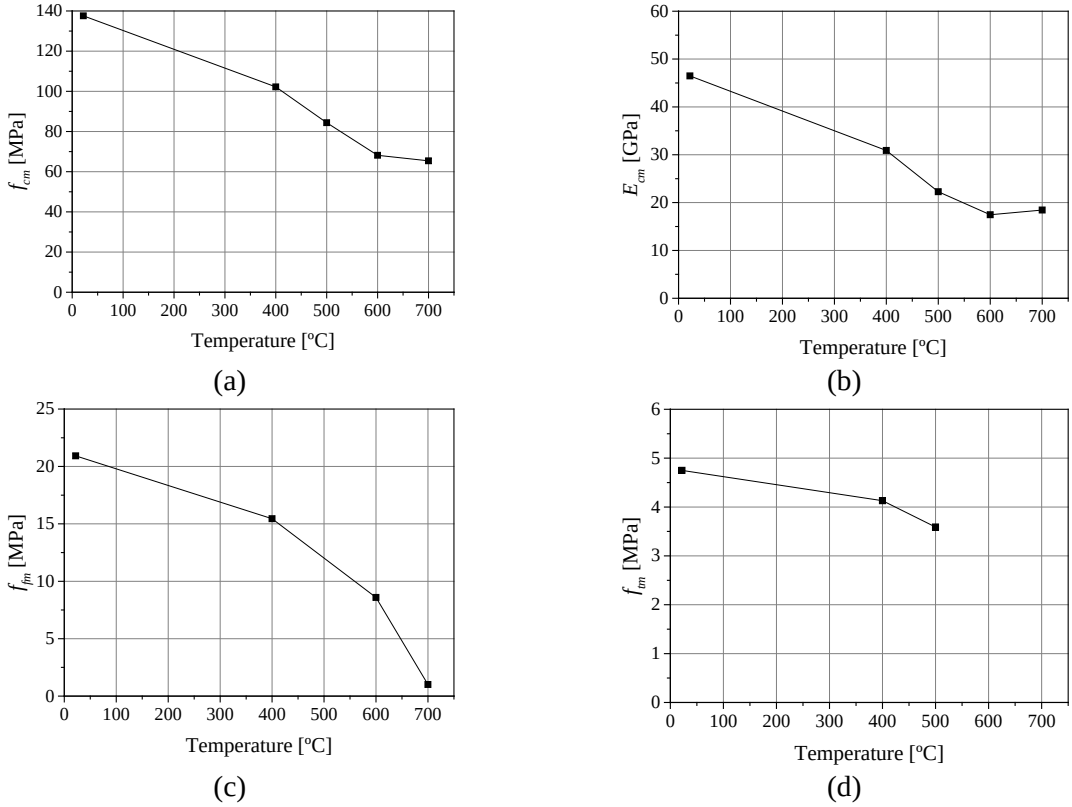

Figure 6. Influence of the temperature on the: (a) compressive strength, (b) modulus of elasticity, (c) flexural strength and (d) tensile strength.

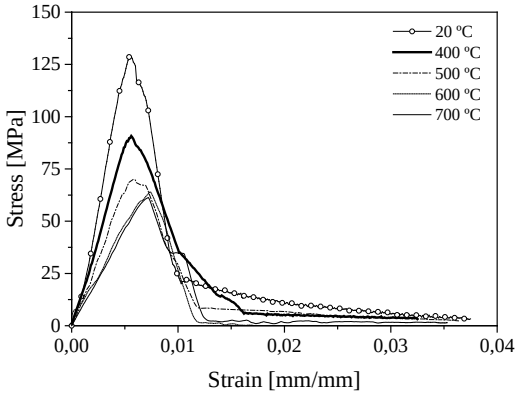

Figure 7. Compressive stress – strain relationships.

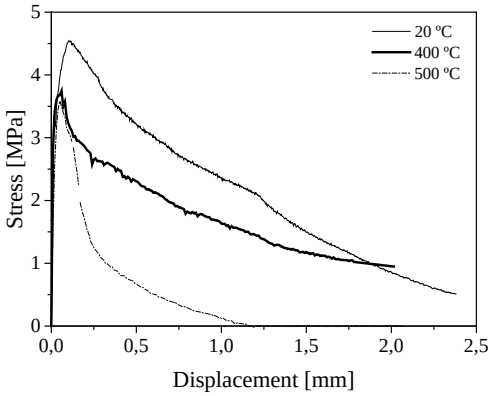

Figure 8. Tensile stress – displacement relationships.

3.2. Tensile stress – displacement relationships

Figure 8 depicts the average tensile stress – displacement curves for the series exposed to distinct temperatures. First of all, it should be noted that the displacement was measured over a gauge length of 120 mm, in the absence of a notch. Therefore, up to the localization of the macro-crack this measure will encompasses the specimen's elastic deformation in the aforementioned region. Since the appearance of multiple cracks was very limited, after the crack localization this displacement can be

roughly regarded as the crack opening width, since the deformation up to this stage will be considerable small. The exposure to temperatures of 400 and 500 ºC did not produced significant changes in the curve's branch up to the peak stress; the decreasing of stiffness in the pre- peak phase for these samples is similar to the stiffness decreasing for compression samples at the same phase. However, the post-peak branches were considerable distinct. In consequence of the significant reduction on the residual tensile strength with temperature, an increase of the slope of the softening branch immediately after tensile strength was also attained, representing the increase of brittleness of the RPC with the temperature. This was related to the thermal induced damage on the matrix that lead to a deterioration of fibre's bond strength and was more significant for the specimens submitted to a temperature of 500 ºC. Moreover, for the latter series, specimens have failed for a very low crack opening width, of about 1.2 mm. On the other hand, the 20 and 400 ºC series, at a deformation of 1.5 mm, still exhibited a considerable residual tensile strength, respectively, about 1.5 and 1.2 MPa.

3.3. Normal stress – deflection relationships under flexure

Figure 9 shows the relationship between the normal stress and deflection obtained in the three-point bending tests. For all specimens, in the pre-peak branch, it is observed a linear branch up to 80 to 90% of the maximum flexural stress followed by a nonlinear branch up to maximum stress. In the post-peak branch a gradual decrease of the residual stress was observed for the series non-exposed to high temperature. The series submitted to 400 and 600 ºC revealed, besides a lower flexural strength, a steeper decrease of the residual flexural strength just after the peak stress was attained. The flexural and residual strength of the series subjected to 700 ºC was very low, and after a deflection higher than 1 mm was practically null.

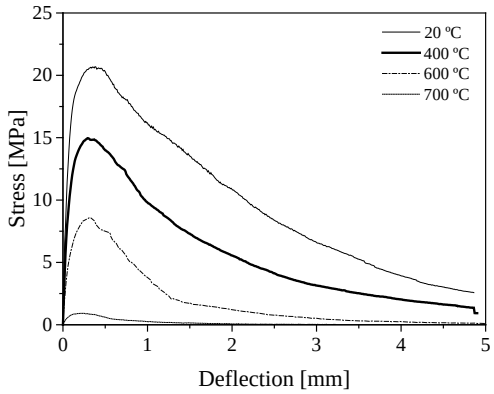

Figure 9. Normal stress – displacement curves under flexure

3.4. Post-cracking parameters

3.4.1. Uniaxial tensile test. The tensile strength, f_{ctm}, stress at crack opening width of 1 and 2 mm, respectively, σ_{1mm} and σ_{2mm}, were computed from the average stress – displacement relationships depicted in figure 8. Additionally, the dissipated energy up to a displacement of 1 and 2 mm, respectively, G_{1mm} and G_{2mm}, were also computed from the latter curves. Figure 10 plots the variation of those parameters with the increase of temperature. In general, the aforementioned parameters decreased with the increase of temperature being the unique exception the small increase of σ_{2mm} from 20 to 400 ºC. Moreover, the decrease of the stresses and dissipated energy at a displacement of 1 and 2 mm were more significant for a 500 ºC temperature. This may be ascribed to a higher pre-induced degree of micro-cracking of the matrix for temperatures higher than 400 ºC, since the dehydration of the calcium hydroxide contributes to the increase of the pore pressure [14]. After this level of temperature, the reinforcement mechanisms provided by fibres are significantly affected detrimentally.

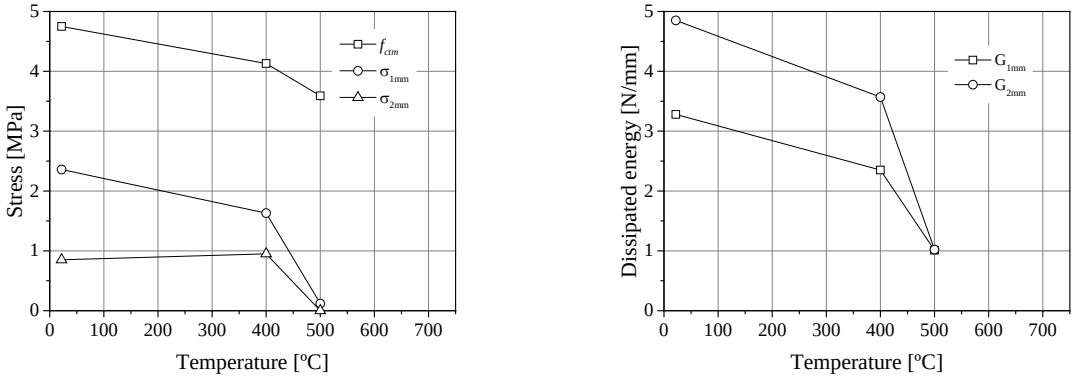

(a) (b)

Figure 10. Influence of the temperature on the tensile post-cracking parameters: (a) f_{ctm}, σ_{1mm} and σ_{2mm}, and (b) G_{1mm} and G_{2mm}.

3.4.2. Three-point bending test. Table 5 includes the influence of temperature on the flexural tensile strengths, which were computed accordingly to the EN-14651 standard [16]. The residual strengths decreased with the increase of temperature, in particular for temperatures higher than 400 ºC. The residual strengths, f_{R1} and f_{R3} are of particular interest for service and ultimate limit state analysis, respectively. For an exposure temperature of 600 ºC, the f_{R1} and f_{R3} faced a reduction of about 63 and 90%, respectively. The smaller decrease of f_{R1} when compared to f_{R3}, may be ascribed to the mobilization of the fibres still being in an initial stage of the fibre pull-out, consequently leading to the mobilization of lower fibre pull-out loads. On the other hand, for f_{R3}, the fibre pull-out is on a much more advanced stage, taking into account that the matrix for this temperature (i.e. 600 ºC) has extensive thermal induced damage, the fibre / matrix bond strength is significantly reduced, therefore the fibres can easily be pulled out for lower loads resulting in a lower crack bridging stress.

Table 5. Flexural tensile strengths obtained from the three-point bending tests.

Temperature	f_{R1} [MPa]		f_{R2} [MPa]		f_{R3} [MPa]		f_{R4} [MPa]	
	Avg.	CoV	Avg.	CoV	Avg.	CoV	Avg.	CoV
20 ºC	20.3	10.1%	13.5	14.9%	8.4	16.5%	5.3	21.6%
400 ºC	14.0	16.9%	7.3	17.0%	4.1	17.2%	2.5	15.9%
600 ºC	7.5	0.0%	1.8	0.0%	0.8	0.0%	0.3	0.0%
700 ºC	0.8	16.2%	0.2	22.3%	0.1	40.5%	0.0	-

4. Conclusions

This work presented and discussed the results of an experimental program to investigate the mechanical behaviour of reactive powder concrete, RPC, reinforced with steel fibres when subjected to high temperatures ranging from 400 to 700 ºC. Based on the experimental results presented in this work, the following main conclusions can be pointed out:

1. RPC specimens could not be fully dried at 60 ºC for a period of 24 hours. For this drying condition, it was observed an explosive spalling failure at a temperature of approximately 450 ºC. On the other hand RPC specimens that have been dried at a temperature of 100 ºC for the same curing period did not exhibit explosive spalling failure, even at 700 ºC temperatures.
2. The compressive, flexural and tensile strength, as well as the elasticity modulus, decreased at a higher rate for temperatures higher than 400 ºC. For an exposure temperature of 600 ºC, the reduction on the compressive strength, elasticity modulus and flexural strength, when compared to the one obtained for room temperature, was about 50, 62 and 60%, respectively. On the other hand, the tensile strength revealed a slight decrease with temperature, however since only it was possible to test specimens exposed up to 500 ºC no definite conclusions can be withdraw.

3. In general, the residual uniaxial tensile strengths and the dissipated energy decreased with the increase of temperature, being the rate of decrease higher for temperatures above 400 ºC.
4. The residual flexural tensile strengths also decreased with the increase of temperature, being also the rate of decrease higher for temperatures above 400 ºC. Moreover, the decrease of f_{R3} with temperature was significantly higher than the one observed for f_{R1}, which could be ascribed to the fibre pull-out being on a much more advanced stage when f_{R3} is evaluated. The reduction of the fibre / matrix bond strength due to the extensive thermal induced micro-cracking enabled the fibres being pulled out for lower loads resulting in a lower crack bridging stresses.

Acknowledgements

The authors would like to acknowledge the Zhejiang Boen Company and MAPEI Company for providing gratuitously, respectively, the steel fibers and micro silica fume. The first author would also like to acknowledge the grant obtained under the scope of the Erasmus Mundus - Marhaba project. The third author wishes to acknowledge the grant SFRH/BSAB/114302/2016 provided by FCT.

5. References

[1] Cheyrezy M, Maret V, and Frouin L, 1995, Microstructural analysis of RPC (reactive powder concrete), *J. Cem. &Con. Res.* **25** 1491–1500.
[2] Bonneau O, Poulin C, Dugat J, Richard P, and Aitcin P C , 1996, Reactive powder concretes: from theory to practice, *J. Con. Inter*. **18** 47-9.
[3] Richard, P and Cheyrezy M H, 1994, Reactive powder concrete with high ductility and 200-800 MPa Compressive Strength, Concrete Technology Past, Present, and Future, ACI SP 144, editor; P. Kumar Mehta, S. Francisco, USA, 507-18.
[4] Shu-hua LIU, Li-hua LI and and Jian-wen FENG, 2012, Study on Mechanical Properties of Reactive Powder Concrete, *J. Civ Eng. &Cons.*, **1:1.** 6-11
[5] Richard P, and Cheyrezy M, 1995, Composition of reactive powder concrete", cement and concrete research, **25(7)**, 1501 –11.
[6] Schneider U, Diederichs U, Horvath J and et al., 2003, Verhalten von ultrahochfesten betonen (uhpc) unter randbeanspruchung (behaviour of ultra-high performance concrete (UHPC) under fire exposure), Beton- und Stahlbetonbau, **98(7)**, 408–17.
[7] Majorana C E and Pesavento F, 2000, Damage and spalling in HP and UHF concrete at high temperature," in Damage and Fracture Mechanics VI: Computer Aided Assessment and Control, vol. 6 of *Structures and Materials*, 105–17.
[8] Ratvio J, 2001, Ultralujan betonin kayttosovellukset Esitutkimus (preliminary study of ultra-strength concrete applications), VTT Tiedotteita, **2078**, 3–45.
[9] Liu C T and Huang J S, 2009, Fire performance of highly flowable reactive powder concrete," *J. Con. & Buil. Mat*., **23(5)**, 2072–79.
[10] Ridha M M S, MohammadAli T Kh, Abbawi Z W, 2013, Behavior of axially loaded reactive powder concrete columns **,** *J. Eng. & Dev.*, **17- 2**, 193-209.
[11] Rahmatabadi M A D, 2015, Mechanical properties of reactive powder concrete under pre-setting pressure and different curing regimes, *J. Str.& Civ. Eng. Res.* **4(4)**, 354-58.
[12] Phan LT., Carino N J, 2001, Mechanical Properties of High Strength Concrete at Elevated Temperatures, Gaithersburg, Maryland: NISTIR 6726, Building and Fire Research Laboratory, National Institute of Standards and Technology,.
[13] Ali F, 2002, Is High Strength Concrete More Susceptible to Explosive Spalling than Normal Strength Concrete in Fire?, *J. Fire Mater.* **26** 127-30.
[14] Zhang Q, Ye G, 2012, Dehydration kinetics of Portland cement paste at high temperature, *J. Ther. Analy. & Cal.* **110**: 153-58.
[15] LNEC E397, 1993. Concretes – Determination of the compressive elasticity modulus. Technical report, National Laboratory for Civil Engineering, Lisboa, Portugal (in Portuguese).
[16] EN 14651, 2005. European Committee for Standardization, Brussels.